

Photometric study of an eclipsing binary in the field of M37

Devarapalli Shanti Priya, Kandulapati Sriram and Pasagada Vivekananda Rao

Department of Astronomy, Osmania University, Hyderabad 500 007, India; *astroshanti@gmail.com*

Received 2013 November 3; accepted 2014 March 24

Abstract CCD photometric observations with B and V passbands were performed on the contact binary V3 in the field of open cluster M37. The solutions were obtained for data from both B and V passbands along with R passband given by Hartman et al. using the Wilson-Devinney code. The positive O'Connell effect was observed in all the three passbands and its associated cool spot parameters were derived. The results indicate that the spot parameters have not shown any significant variability during the last four years. The spot radius was found to be 40° and located close to the equator of the secondary component. The absolute parameters of the system were derived using the empirical relations given by Gazeas et al.

Key words: binaries: eclipsing — binaries: close

1 INTRODUCTION

The study of contact binaries gives insight into stellar evolution theory, through fundamental stellar parameters like mass, radius, luminosity and composition (Yakut & Eggleton 2005). These binaries have short periods (≤ 1 d) and hence are suitable for studying the mechanism of merging and may explain progenitors such as stars like FK Comae Berenices, blue stragglers etc. Moreover, among contact binaries, few of them exhibit the O'Connell effect (O'Connell 1951) and their variability may provide a clue to the magnetic cycle prevailing in the system (Qian et al. 2007). Furthermore, some long term studies of contact binaries have revealed the presence of a third body (Rucinski et al. 2007; Pribulla & Rucinski 2006).

The open cluster M37 (NGC 2099) has been surveyed for variable stars (Kiss et al. 2001; Kang et al. 2008) and a total of 1454 variable stars were discovered (Hartman et al. 2008) among which 11 were contact binary systems. One of the contact binary systems (labeled as ID V3) was selected for our photometric study as it was relatively bright ($V_{\max} \sim 15.6$) and had a pronounced instance of the O'Connell effect. Detailed B , V and R passband photometric solutions were obtained using the Wilson-Devinney code (Wilson & Devinney 1971; van Hamme & Wilson 2003).

2 OBSERVATIONS AND DATA REDUCTION

CCD photometric observations of the variable were carried out using the 2 m telescope at IUCAA Girawali Observatory, India. The observations were performed for six nights on 2011 February 24–27 and 2011 November 29 and 30. The IUCAA Faint Object Spectrograph Camera (IFOSC) equipped with an EEV $2K \times 2K$ thinned, back-illuminated CCD with a pixel size of $13.5 \mu\text{m}$ was used, which provided an effective field view of $\sim 10' \times 10'$ on the sky corresponding to a plate scale of $0.3''$ per pixel. The field was centered at $\alpha_{J2000} = 05^{\text{h}} 52^{\text{m}} 33.01^{\text{s}}$, $\delta_{J2000} = 32^\circ 32' 42.00''$ and totals

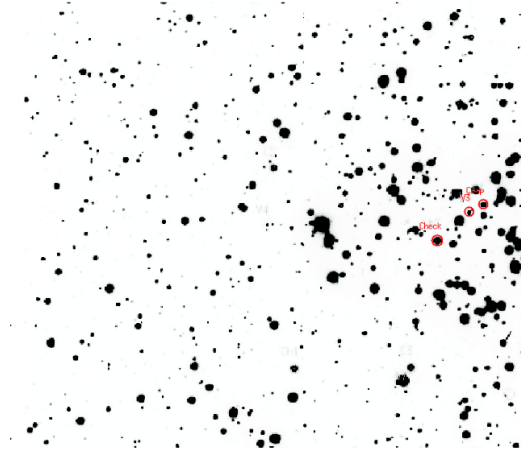


Fig. 1 $\sim 10' \times 10'$ image of the field of NGC 2099. The variable (V3), comparison (C1) and check (C2) stars are marked.

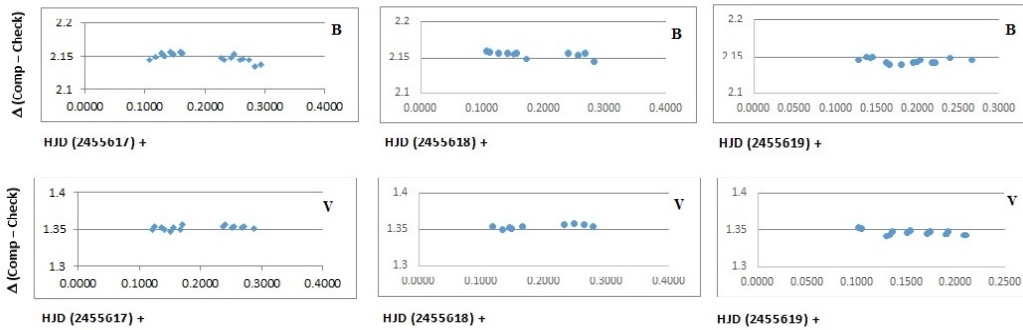


Fig. 2 Magnitude difference between comparison and check star for three nights in the B and V passbands.

of 158 frames in the B band and 71 frames in the V band were obtained with an exposure time of 600 s. The aperture photometry was performed with the *apphot* package available in IRAF software.

Figure 1 shows the positions of the variable (V3), comparison (C1) and check (C2) stars. Figure 2 shows the light curve Δm (comparison-check) (~ 0.02) vs. HJD, which remains constant over the period of our observations. The observed variable light curve shows a shape similar to the one published by Hartman et al. (2008). The phases were calculated using the following ephemeris

$$\text{HJD MinI} = 2455619.1516 + 0.42248^d \times E(B \text{ passband}).$$

3 PHOTOMETRIC SOLUTIONS

The details of the variable V3 are listed in Table 1. Initially mode 2 of the Wilson–Devinney code was adopted, which later converged to mode 3. The procedure adopted for fixing the primary star (hot)

temperature, gravity-darkening coefficients g_h and g_c and albedos A_h and A_c for the components was similar to that described in our earlier papers (Sriram et al. 2009; Sriram & Vivekananda Rao 2010; Shanti Priya et al. 2011, 2013a,b; Ravi Kiron et al. 2011a,b, 2012). The primary temperature was fixed after correcting the observed $B - V$ (Cox 2000). The relation $(B - V)_0 = (B - V) - E(B - V)$ was used, where $E(B - V) = A_V = R \times E(B - V)$. The values of A_V (Hartman et al. 2008) and R were fixed at 1.18 and 3.1 respectively. The wavelengths were fixed at 4455 Å and 5497 Å for the B and V passbands respectively and their corresponding limb-darkening coefficients were taken as $x_h = 0.610$ and $x_c = 0.549$. The following parameters were considered as adjustable parameters: the effective temperature of the secondary component T_c , the dimensionless surface potentials $\Omega_h = \Omega_c$, mass ratio (q) and the monochromatic luminosity L_h along with orbital inclination i . The procedure was repeated until a minimum weighted sum of square of residuals ($\Sigma w(o - c)^2$) was attained.

Table 1 Details of Variable V3

Star ID	Period (d)	V	$B - V$	Temperature (K)	Spectral type
V3	0.442483	16.051	0.728	7018	F2–F0

Figure 3 shows q versus $(\Sigma w(o - c)^2)$ with a minimum at $q = 1.28 \pm 0.06$. A similar procedure resulted in $q = 1.22 \pm 0.04$ from the R passband data. The theoretical solutions were fitted to the observed light curves and large residuals around phase 0.75 were noticed (Figs. 4 and 5). In order to improve the fit, a cool spot on the secondary was added and this resulted in small residuals (Figs. 4 and 5). To check the consistency of the solutions, the temperature of the primary component was varied by $\pm 100 - 200$ K but no significant changes in the solution were noticed.

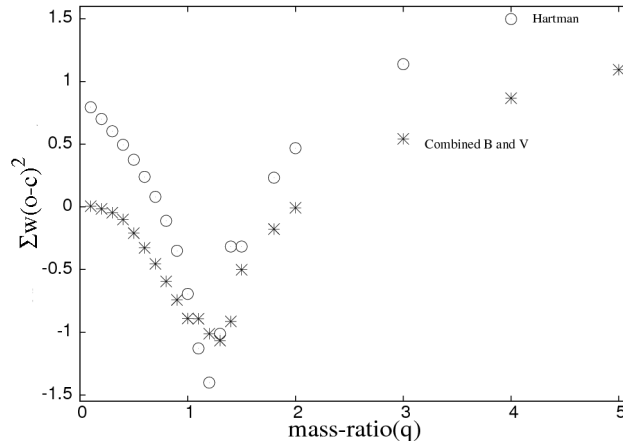


Fig. 3 q vs. $\Sigma w(o - c)^2$ for B , V (our observations) and R passbands (Hartman et al. data).

4 DISCUSSION AND RESULTS

A visual inspection of the light curves from the B , V and R passbands of V3 indicated W UMa type variability and the W-D code was used to model the light curves shown in Figures 4 and 5. A temperature difference of 700 K was observed between the primary and secondary components (see Table 2), suggesting that variable V3 is not in thermal contact. The values of q and i were found to be ~ 1.28 and $\sim 63^\circ$ using data from the B and V passbands, and ~ 1.22 and $\sim 63^\circ$ using data from the

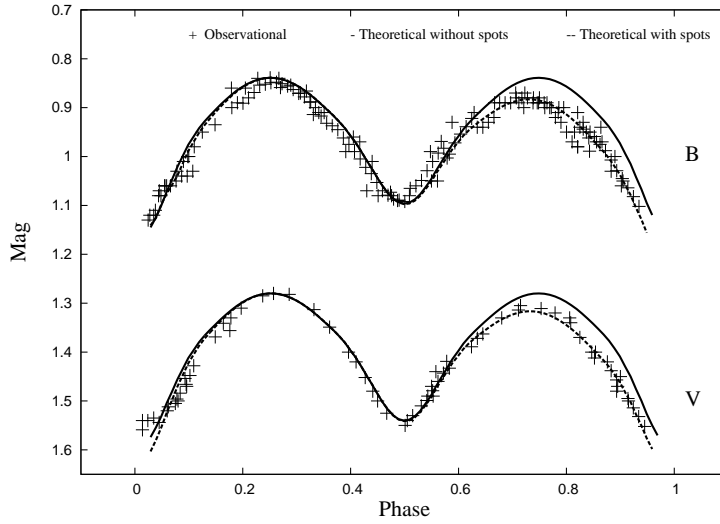


Fig. 4 Best fit of spot and unspotted solutions for light curves from the *B* and *V* passbands.

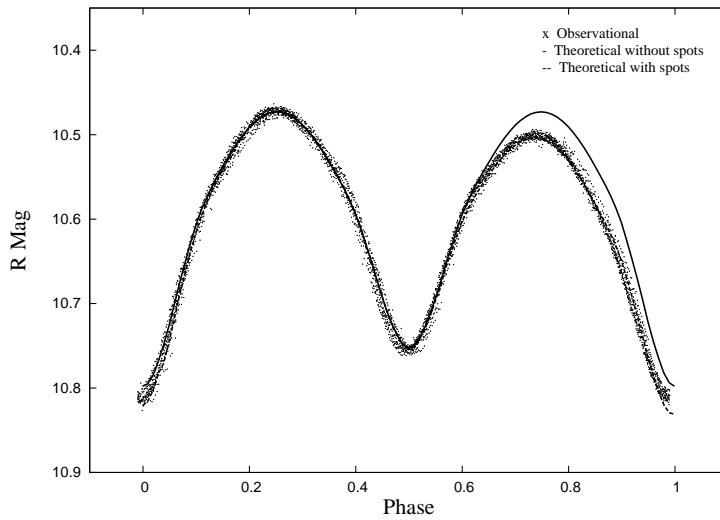


Fig. 5 Best fit of spot and unspotted solutions for light curves from the *R* passband.

R passband. In our light curves, a positive O'Connell effect was observed and a similar feature was also present in the *R* passband (Hartman et al. 2008). Many contact binaries (BB Peg, AG Vir, SW Lac, UX Eri, XY Leo, GM Dra) exhibit this effect, which is observed as an asymmetry in the light curve around phases 0.25 and 0.75. In general, the O'Connell effect is associated with a cool spot on one of the components in the binary system (Kalomeni et al. 2007), however, other possibilities such as hot regions like faculae, gas streams between the stars or some unknown homogeneity cannot be ruled out (Yakut & Eggleton 2005). From our analysis, the radius of the spot was found to be around $\sim 40^\circ$, located at a lower latitude ($\sim 22^\circ$), and its temperature is slightly less than its surroundings (Table 2).

Table 2 The photometric parameters obtained for V3 by using the Wilson-Devinney method.

Element		V3 _{B,V} (Combined)	V3 _R (Hartman)
*T _h (K)		7018	7018
T _c (K)		6386±177	6558±23
q		1.28±0.06	1.22±0.04
i (°)		62.60±0.14	63.42±0.16
Ω		4.2906±0.0634	4.0845±0.0045
fill-out factor		0.1188	0.0288
r _h	pole	0.3344±0.0074	0.3410±0.0005
	side	0.3502±0.0090	0.3576±0.0006
	back	0.3819±0.0133	0.3899±0.0009
r _c	pole	0.3781±0.0070	0.3742±0.0005
	side	0.3985±0.0088	0.3943±0.0006
	back	0.4285±0.0123	0.4252±0.0008
L _h	B	0.5599	0.5128
	V	0.5208	
L _c	B	0.4401	0.4872
	V	0.4792	
*A _h		0.5	0.5
*A _c		0.5	0.5
*G _h		0.32	0.32
*G _c		0.32	0.32
Σw(o - c) _{Unspotted} ²		0.2003	0.0055
Spot parameters			
* Co-latitude (Ø°)		68.75	68.75
Longitude (θ°)		236.42±6.20	229.81±2.00
Spot Radius (γ°)		42.42±5.12	38.38±3.38
Temp. Factor		0.92±0.08	0.94±0.01
Σw(o - c) _{Spotted} ²		0.1277	0.0002

Notes: $L_h + L_c = 1$ and * fixed parameter.

As the radius of the spot is large, we assume that it would survive for a longer duration and consequently may show a variable O'Connell effect like, for example, BX Peg (Lee et al. 2004), AD Cnc (Qian et al. 2007), FG Hya (Qian & Yang 2005), etc. For some systems, the observed asymmetry in light curves is persistent, like in BB Peg, where the cool spot varies in size and location but does not show any activity cycle over a period of ~25 yr (Kalomeni et al. 2007). In another contact binary system CC Com, authors have found the appearance and disappearance of the spot over a duration of ~35 yr (Köse et al. 2011). From the present study, the location and size of the spot have not shown any significant variation and hence we conclude that the spot is persistent over a period of four years. To understand variations in the spot parameters and their associated activity cycle, further observations are needed.

Gazeas (2009) derived a three dimensional empirical correlation using data from several contact binary systems and these relations are given below:

$$\log M_h = 0.725 \log P - 0.076 \log q + 0.365 ,$$

$$\log M_c = 0.725 \log P + 0.924 \log q + 0.365 ,$$

$$\log R_h = 0.930 \log P - 0.141 \log q + 0.434 ,$$

$$\log R_c = 0.930 \log P + 0.287 \log q + 0.434 ,$$

$$\log L_h = 2.531 \log P - 0.512 \log q + 1.102 ,$$

$$\log L_c = 2.531 \log P + 0.352 \log q + 1.102 .$$

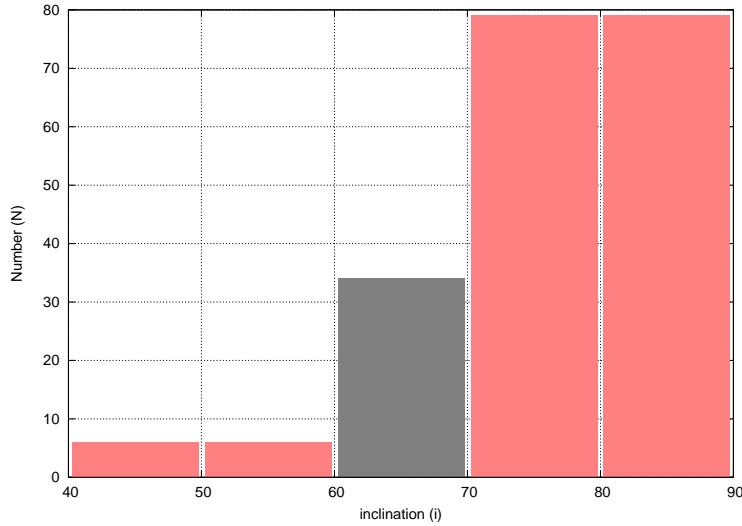


Fig. 6 Histogram of the inclination of contact binaries (see text). The grey shaded region highlights the inclination of contact binaries between 60° – 70° . The derived inclination of variable V3 lies in this region.

Substituting the mass ratio and period, we derived the following parameters for the variable V3: $M_h = 1.26 M_\odot$, $M_c = 1.61 M_\odot$, $R_h = 1.23 R_\odot$, $R_c = 1.37 R_\odot$, $L_h = 1.42 L_\odot$ and $L_c = 1.75 L_\odot$.

The theoretical solutions obtained from *BVR* passbands indicate that V3 is a partially eclipsing contact binary ($i \sim 63^\circ$).

Figure 6 shows a histogram where there are several contact binaries with similar inclinations. The data for the histogram were compiled from Pribulla et al. (2003) and the references therein, Deb & Singh (2011) and Fang et al. (2013), whose solutions were obtained from either only photometry or also including spectroscopy.

We suggest long term monitoring of variable V3 be performed using both photometry and spectroscopy in order to study the long term inherent magnetic cycle associated with the secondary, based on the behavior of the spot, and to check the reliability of our results.

Acknowledgements The authors thank the director of IUCAA, Pune for allocating telescope time and Dr. Vijay Mohan for helping us with the observations. We also acknowledge Dr. J. D. Hartman for providing the *R* passband data for the variable V3. We thank the anonymous referee for comments which improved the quality of the paper.

References

- Cox, A. N. ed. 2000, *Allen's Astrophysical Quantities* (4th ed.; Berlin: Springer)
- Deb, S., & Singh, H. P. 2011, *MNRAS*, 412, 1787
- Fang, X.-S., Gu, S.-H., Zhang, L.-Y., & Pi, Q.-F. 2013, *RAA (Research in Astronomy and Astrophysics)*, 13, 1052
- Gazeas, K. D. 2009, *Communications in Asteroseismology*, 159, 129
- Hartman, J. D., Gaudi, B. S., Holman, M. J., et al. 2008, *ApJ*, 675, 1233
- Kalomeni, B., Yakut, K., Keskin, V., et al. 2007, *AJ*, 134, 642

- Kang, Y. B., Kim, S.-L., Rey, S.-C., et al. 2008, *PASP*, 120, 358
- Kiss, L. L., Szabó, G. M., Sziládi, K., et al. 2001, *A&A*, 376, 561
- Köse, O., Kalomeni, B., Keskin, V., Ulaş, B., & Yakut, K. 2011, *Astronomische Nachrichten*, 332, 626
- Lee, J. W., Kim, C.-H., Han, W., Kim, H.-I., & Koch, R. H. 2004, *MNRAS*, 352, 1041
- O'Connell, D. J. K. 1951, *Publications of the Riverview College Observatory*, 2, 85
- Pribulla, T., Kreiner, J. M., & Tremko, J. 2003, *Contributions of the Astronomical Observatory Skalnaté Pleso*, 33, 38
- Pribulla, T., & Rucinski, S. M. 2006, *AJ*, 131, 2986
- Qian, S., & Yang, Y. 2005, *MNRAS*, 356, 765
- Qian, S.-B., Yuan, J.-Z., Soonthornthum, B., et al. 2007, *ApJ*, 671, 811
- Ravi Kiron, Y. R., Sriram, K., & Vivekananda Rao, P. 2011a, *Bulletin of the Astronomical Society of India*, 39, 247
- Ravi Kiron, Y. R., Sriram, K., & Vivekananda Rao, P. 2011b, *RAA (Research in Astronomy and Astrophysics)*, 11, 1067
- Ravi Kiron, Y. R., Sriram, K., & Vivekananda Rao, P. 2012, *Bulletin of the Astronomical Society of India*, 40, 51
- Rucinski, S. M., Pribulla, T., & van Kerkwijk, M. H. 2007, *AJ*, 134, 2353
- Shanti Priya, D., Sriram, K., & Vivekananda Rao, P. 2011, *RAA (Research in Astronomy and Astrophysics)*, 11, 175
- Shanti Priya, D., Sriram, K., & Vivekananda Rao, P. 2013a, *RAA (Research in Astronomy and Astrophysics)*, 13, 465
- Shanti Priya, D., Sriram, K., Shaju, K. Y., & Vivekananda Rao, P. 2013b, *Bulletin of the Astronomical Society of India*, 41, 159
- Sriram, K., Ravi Kiron, Y. R., & Vivekananda Rao, P. 2009, *RAA (Research in Astronomy and Astrophysics)*, 9, 1149
- Sriram, K., & Vivekananda Rao, P. 2010, *RAA (Research in Astronomy and Astrophysics)*, 10, 159
- van Hamme, W., & Wilson, R. E. 2003, in *GAIA Spectroscopy: Science and Technology*, *Astronomical Society of the Pacific Conference Series*, vol. 298, ed. U. Munari, 323
- Wilson, R. E., & Devinney, E. J. 1971, *ApJ*, 166, 605
- Yakut, K., & Eggleton, P. P. 2005, *ApJ*, 629, 1055